Macromolecules

pubs.acs.org/Macromolecules
Article

Tuning the Adhesive Strength of Functionalized Polyolefin-Based Hot Melt Adhesives: Unexpected Results Leading to New Opportunities

Jakub Kruszynski,[¶] Weronika Nowicka,[¶] Farhan Ahmad Pasha, Lanti Yang, Artur Rozanski, Miloud Bouyahyi, Ralf Kleppinger, Lidia Jasinska-Walc,* and Rob Duchateau*

Cite This: https://doi.org/10.1021/acs.macromol.4c02945

ABSTRACT: The development of lightweight, often multicomponent products requires adaptable and robust bonding solutions. Hot melt adhesives increasingly attract industrial interest as they combine good adhesive strength, facile processability, and cost-efficiency. Recently, our group has reported on the remarkable adhesive performance of hydroxyl-functionalized propylene-based copolymers in bonding both polar and nonpolar surfaces. The obtained adhesive strength proved to be too high for applications such as single-use packaging, which requires low to moderate adhesion for easy opening. Tuning the adhesive strength by manufacturing numerous functionalized polyolefin grades with varying contents of hydroxyl-functional groups is challenging in view of industrial-scale production. Herein, we elucidate an alternative approach to tune the adhesive performance by blending the functionalized propylene copolymers with nonfunctionalized congeners. To understand the structure−property relationship of the investigated diluted blends, a thorough characterization of morphology, physical properties, crystallization, and viscoelastic behavior was performed. It appeared that the crystallinity of the nonfunctionalized polyolefin and its miscibility with the functionalized polyolefin play a crucial role on the adhesive strength of the blends. Either a gradual decrease in adhesive strength with dilution was noticed or—surprisingly—no loss of adhesive strength was observed at all, not even after diluting 100 times! Molecular dynamics simulations revealed an intrinsic tendency of the hydroxyl-functionalized polyolefin to migrate to and interact with the aluminum oxide surface.

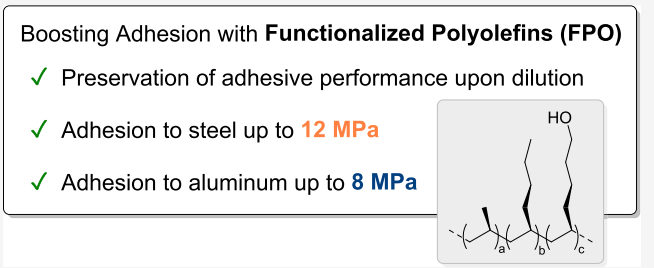

INTRODUCTION

Adhesives have been vital since the dawn of civilization and remain essential across many fields in our daily life. Their importance continues to grow as technology advances, making them fundamental to the development of new hybrid materials and products. Many applications demand specialized bonding technologies and precise formulations, resulting in a wide range of adhesive types.[1−4] These include solvent-based systems, adhesive melts, reactive adhesives like UV- or water-curable systems, and nonreactive thermoplastics.[5,6]

Hot melt adhesives (HMAs) become increasingly important due to their environmentally friendly profile compliant with low VOC emission regulations, excellent properties, simple application, and low costs.[3] So far, commercially available HMAs have been dominated by EVA-based solutions and polyurethanes, while polyolefin elastomers (POEs) gradually gain market share in certain applications like building and construction, packaging, and the automotive industry.[7,8] For high-performance applications, typically reactive HMAs are applied as chemical cross-linking is required to ensure sufficient adhesive strength.[5]

Driven by the desire to debond substrates after use for improved recyclability, nonreactive high strength HMAs are being searched for. For example, Sun et al.[9] developed a bisphenol A-based polyether-amine with dynamic noncovalent bonds (DCBs), while Saito and co-workers[10] reported on borate ester-based adhesives having DCBs that showed excellent adhesion to steel.

Recently, our group has reported on the unprecedented high adhesive strength of randomly functionalized propylene-based copolymers, namely, poly(propylene-*co*-hex-1-ene-*co*-hex-5-en-1-ol) (poly(C_3−C_6−C_6OH)), to both polar and nonpolar substrates, *viz*., aluminum, steel, glass, wood, and *i*PP.[2,11] We argued that by tuning the adhesive strength of these functionalized polyolefins, we could obtain a simple sustainable

Received: November 28, 2024
Revised: January 16, 2025
Accepted: February 24, 2025

https://doi.org/10.1021/acs.macromol.4c02945
Macromolecules XXXX, XXX, XXX−XXX

HMA solution for a wide range of market segments ranging from durable building and construction and automotive and transportation industries—requiring high adhesive strength—to single-use end-of-line packaging and personal hygiene for which a significantly lower adhesive strength is essential. Here, we describe the results of our study on tuning the adhesive strength of functionalized polyolefin-based HMA systems by either varying the functionality level of the functionalized polymers or by diluting functionalized polyolefins with nonfunctionalized congeners.[12]

RESULTS AND DISCUSSION

Adhesion of polymers is a complex matter and numerous mechanisms portray the complexity of the bonding process, including diffusion of the adhesive into polymer substrates, interlocking on rough surfaces and chemical interactions of functional groups with polar surfaces.[13] Although the strength of the chemical bonds typically contributes to only a small fraction of the final adhesive strength, it is believed that increasing the functionality level of the functionalized polyolefin enhances the adhesive strength. To confirm this, we have prepared functionalized propylene-based copolymers with varying levels of randomly distributed short chain branches (SCBs) and hydroxyl functionalities, and we have applied these polymers as single-component HMAs for gluing aluminum and steel. Well-defined hydroxyl-functionalized propylene-based elastomers, poly(C_3−C_6−C_6OH) with hex-1-ene and hex-5-en-1-ol levels ranging from 9 to 10 mol % and 0.1 to 0.5 mol %, respectively, and weight-average molecular weights in the range of 140 to 200 kg·mol^{-1} were synthesized by copolymerization of propylene, hex-1-ene, and triethylaluminum-passivated hex-5-en-1-ol (Figure 1, Table 1 A−C).

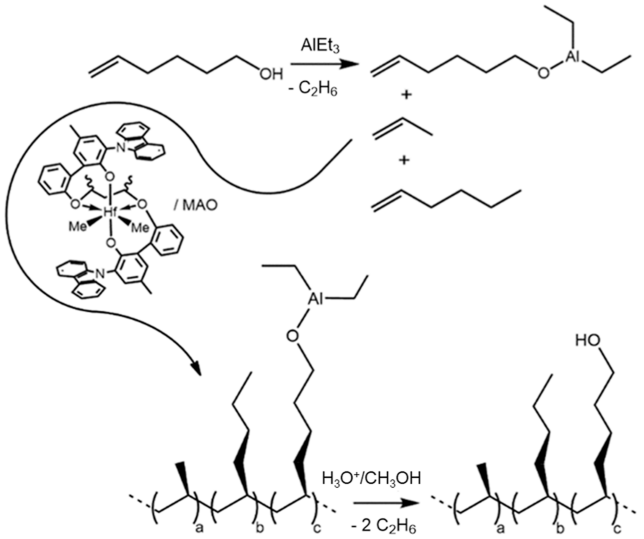

Figure 1. Synthetic path toward poly(C_3−C_6−C_6OH).

Corresponding nonfunctionalized poly(propylene-*co*-hex-1-ene) (poly(C_3−C_6); Table 1, D, E) elastomers containing 7 to 9 mol % of hex-1-ene were synthesized as well and were used as a benchmark together with commercially available poly(propylene-*co*-but-1-ene) (poly(C_3−C_4)) and poly(propylene-*co*-ethylene) (poly(C_3−C_2)) elastomers (Table 1, F, G), with 17 mol % and 19 mol % of the comonomer, respectively.

The incorporation level of hex-5-en-1-ol into the polymer backbone was determined by ^{1}H NMR spectroscopy using the −CH_2−OH resonance signals at around 3.5 ppm (Table S1, Figures S1 and S2). The introduction of randomly distributed butyl branches provided materials with suppressed crystallinities and melting transitions when compared with isotactic polypropylene (Figure 2). The targeted melting temperature (T_m) of the copolymers determined by Differential Scanning Microscopy (DSC) was around 80 °C (Tables S1 and S2, Figure S3). Glass transition temperatures (T_g) of the materials, determined by Dynamic Mechanical Thermal Analysis (DMTA), are typical for propylene-rich copolymers and were recorded in the range from −3 to 0 °C, except for the poly(C_3−C_2) benchmark material, revealing a T_g of −19 °C (Table 1).

Adhesion Performance of Functionalized Polyolefins. The adhesion performance of poly(C_3−C_6−C_6OH) samples **A**−**C** containing 0.5 mol %, 0.4 mol %, and 0.1 mol % of hex-5-en-1-ol, respectively, was compared with nonfunctionalized poly(C_3−C_x) (x = 2, 4, 6) copolymers **D**−**G**. The adhesive strength was measured by performing Lap Shear Strength (LSS) tests, a facile and standardized technique especially for performance screening purposes.[14−18] Functionalized polyolefins **A**−**C** demonstrated seriously stronger adhesion to aluminum and steel when compared to the nonfunctionalized reference samples **D**−**G** (Table 1, Figure 3). As anticipated, the sample having the highest hydroxyl functionality per chain provided the highest adhesive strength. Increasing the polyolefin functionality level from 0.1 to 0.5 mol % resulted in a nearly three times higher adhesion to aluminum up to 7.7 MPa. A similar trend was observed for the steel lamination where the adhesion strength exceeded 14 MPa for sample **A**. As already indicated, these adhesive strengths are orders of magnitude higher than the maximum bond strength of the chemical interactions. Assuming a coverage of 5 oxide/hydroxide groups per nm^2 on the aluminum oxide surface that could react with the functionalized polyolefin's hydroxyl functionality,[19] the maximum strength of the sum of the chemical interactions is approximately 30 kPa, which is 3 orders of magnitude lower than the observed adhesive strength.[13] Keeping in mind that adhesion is a complex property governed by numerous factors, such as wettability, viscosity, and entanglements, the adhesive contribution (component) of functional groups is minute yet requisite for efficient bonding.

One of the clear advantages of producing functionalized polyolefins by catalysis is the flexibility of the process allowing tailoring of various polymer properties including the hydroxyl functionality level and thereby their adhesion strength. Although easily applicable on a lab scale, for the commercial manufacturing of such products, changing the functionality level by tuning the functionalized comonomer feed conditions will result in significant amounts of off-spec material during grade transitions in the reactor. We envisioned that diluting functionalized polyolefins with a nonfunctionalized polyolefin might be an easier and economically more viable approach to tune the adhesive strength of the functionalized polyolefin.

To investigate this hypothesis, sample **B** was selected to prepare blends with several nonfunctionalized propylene-based POEs: low- and a high-molecular-weight unfunctionalized congeners of **B** (poly(C_3−C_6) (**D**, **E**)) and two commercially available propylene copolymers, poly(C_3−C_4) (**F**; TAFMER, Mitsui Chemicals) and poly(C_3−C_2) (**G**; Vistamaxx, Ex-

https://doi.org/10.1021/acs.macromol.4c02945
Macromolecules XXXX, XXX, XXX−XXX

Table 1. Molecular Weight, Thermal Properties, and Adhesive Strengths of Poly(C_3−C_6−C_6OH), Poly(C_3−C_6), Poly(C_3−C_4), and Poly(C_3−C_2) Samples

entry	composition	$\bar{M}_n$[a], kg·mol^{-1}	$\bar{M}_w$[a], kg·mol^{-1}	$Đ_M$[a]	C_6OH[b], mol %	T_m[c], °C	T_g[d], °C	Al LSS[e], MPa	steel LSS[f], MPa
A	poly(C_3−C_6−C_6OH)	57.6	208.7	3.6	0.5	81.2	0	n.a[g]	14.5 ± 1.1
B	poly(C_3−C_6−C_6OH)	51.2	204.8	4.0	0.4	77.7	−1	7.7 ± 0.7	11.2 ± 1.0
C	poly(C_3−C_6−C_6OH)	37.8	140.7	3.7	0.1	76.6	0	2.7 ± 0.6	5.8 ± 0.8
D	poly(C_3−C_6)	25.7	78.5	3.1		85.9	0	1.1 ± 0.3	2.0 ± 0.2
E	poly(C_3−C_6)	203.4	752.6	3.7		80.5	−1	1.7 ± 0.5	0.8 ± 0.8
F	poly(C_3−C_4)	119.8	270.1	2.3		78.2	−3	1.6 ± 0.3	1.6 ± 0.4
G	poly(C_3−C_2)	117.4	258.2	2.2		106.0	−19	1.3 ± 0.2	0.9 ± 0.3

[a]Determined by HT-SEC in 1,2-dichlorobenzene at 150 °C. [b]Hex-5-en-1-ol content, determined by ^{1}H NMR. [c]Determined by DSC. [d]Determined by DMTA. [e]Aluminum/aluminum lap shear strength. [f]Steel/steel lap shear strength. [g]Aluminum substrate failure.

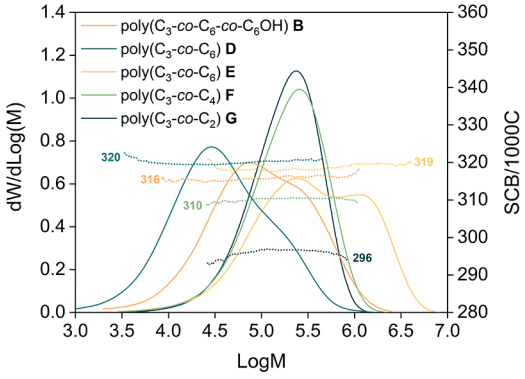

Figure 2. High-Temperature-Size Exclusion Chromatography (HT-SEC) and SCB analysis of poly(C_3−C_6−C_6OH) sample **B**, non-functionalized poly(C_3−C_6) sample **D**, **E**, poly(C_3−C_4) sample **F**, and poly(C_3−C_2) sample **G**.

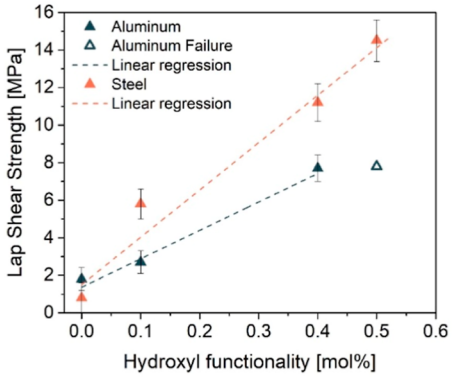

Figure 3. Lap shear test results of the poly(C_3−C_6−C_6OH) samples: **A** (C_6OH mol % = 0.5), **B** (C_6OH mol % = 0.4), and **C** (C_6OH mol % = 0.5) compared with nonfunctionalized poly(C_3−C_6) sample **D**.

xonMobil). Sample **B** was chosen for this study as the adhesive strength of sample **A** was too high to be determined for aluminum specimen as aluminum substrate failure occurred. By blending **B**, revealing a moderate functionality level, with varying amounts of a nonfunctionalized propylene-based POE, a product with a tunable average hex-5-en-1-ol content between 0 and 0.4 mol % was obtained (Figure S2). For each product combination (**B**/**D**, **B**/**E**, **B**/**F**, and **B**/**G**), blend compositions containing either 70, 50, 30, 10, 5, or 1 wt % of the functionalized polyolefin **B** (Tables S1 and S2) were studied. The blends were characterized and subsequently subjected to LSS tests.

Blend Characterization. First, the morphology and physical properties of the blends were thoroughly examined. Transmission Electron Microscopy (TEM) micrographs (Figure 4) of the blends (30:70 w/w) consisting of poly(C_3−C_6−C_6OH) and either poly(C_3−C_6) or poly(C_3−C_4) reveal excellent miscibility of the blend components, whereas comparable 30:70 w/w compositions comprising poly(C_3−C_6−C_6OH) and poly(C_3−C_2) clearly exhibit a two-phase system. Though, the presence of a rough interphase suggests partial interdiffusion of the amorphous phases of each of the latter blend components in the **B**/**G** blend, evincing some degree of miscibility. The investigated compositions reveal a fine-crystalline structure with crystal thickness oscillating around 2−3 nm. These results were also confirmed by Atomic Force Microscopy (AFM) analysis (Figure S4).

As anticipated, the physical properties of the thus prepared blends (**B**/**D**, **B**/**E**, **B**/**F**, and **B**/**G**) are dependent on their composition. While T_m and X_c of the investigated alloys fall within the values set by the pristine components, the T_c of the blends depends on their composition (Table S1 and Figures 5, S5, and S6). The well-miscible blends **B**/**D** and **B**/**E** comprising poly(C_3−C_6−C_6OH) and poly(C_3−C_6) reveal higher T_c (even above 20 °C) when compared to the reference copolymer (Figure 5A,B). This phenomenon can be explained by the similarities of the polymers' crystal structure and epitaxial crystal growth.[20] Clearly, the interactions between the individual blend components and their similarity stabilize the crystalline structure and improve molecular alignment and packing, raising the crystallization temperature of the blend above that of individual polymers. Conversely, the differences of the chemical structure and thus topology between poly(C_3−C_6−C_6OH) and poly(C_3−C_4) (blends **B**/**F**) resulted in a significant decrease of the T_c of up to 40 °C for the corresponding blend (Figure 5C). Although TEM and AFM micrographs of this blend composition do not reveal significant phase separation, the differences of the interplanar distances between polymer chains within poly(C_3−C_4) and the functionalized copolymer (vide infra) clearly decrease their crystallization temperature. The thermal properties and crystallinity level of the **B**/**G** blends (Figure 5D) are governed by the semicrystalline poly(C_3−C_6−C_6OH) component as **G** is essentially amorphous (Tables S1 and S2).

DMTA studies of the polymer blends **B**/**D**, **B**/**E**, and **B**/**F** show single glass transition temperatures in the range of −3 to 4 °C (Table S1, Figure S7). In the **B**/**G** blends, revealing more distinct morphologies and containing up to 10 wt % of functionalized polyolefin **B**, a single T_{g1} deriving from component **G** is visible at −19 °C. Upon reaching 30 wt % of component **B**, the second tan δ peak T_{g2} appears around 0

https://doi.org/10.1021/acs.macromol.4c02945
Macromolecules XXXX, XXX, XXX−XXX

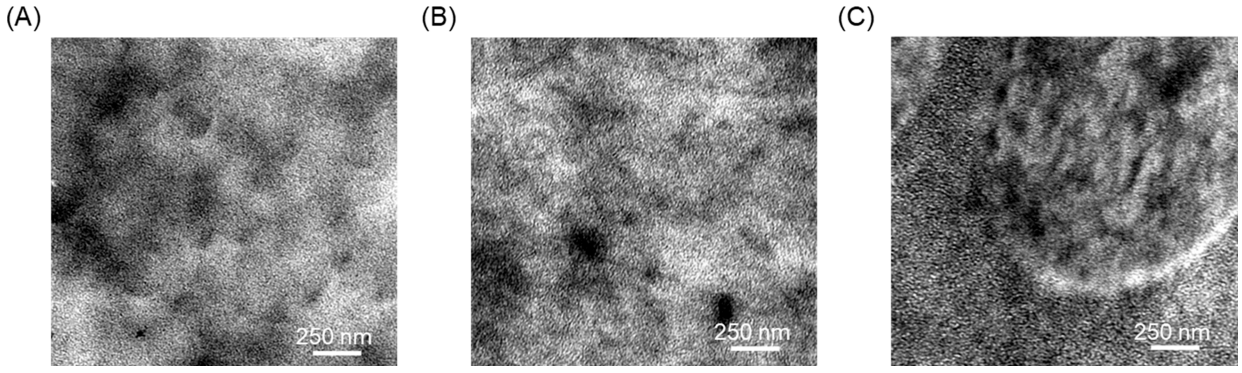

Figure 4. TEM analysis of the 30/70 w/w blend comprising (A) poly(C_3–C_6–C_6OH)/poly(C_3–C_6) (**30B/70D**), (B) poly(C_3–C_6–C_6OH)/poly(C_3–C_4) (**30B/70F**), and (C) poly(C_3–C_6–C_6OH)/poly(C_3–C_2) (**30B/70G**).

°C. Interestingly, with an increasing concentration of **B**, the distance between the two distinct glass transitions increases. As presented in Table 1, the T_{g1} decreases from −19 to −22 °C, while T_{g2} increases from 0 to 3 °C in **30B/70G** and **70B/30G**, respectively. Lehman and co-workers have reported a comparable trend, where the T_g of polypropylene was decreasing with an increasing amount of the amorphous component. Evidently, that deflection of the T_g derives from the amplification of the negative pressure related to the differential thermal coefficients of the blend components.[21] Furthermore, selected elastomers **E** and **F** exhibit stable moduli above the melting point, which clearly differentiates their behavior from that of the functionalized polyolefin **B** and low-molecular-weight nonfunctionalized copolymer **D**. As presented in Figure S7, blending **B** with relatively high-molecular-weight **E** and **F** translates to improved deformation resistance above the melting point, which is the result of increased entanglement next to the network formed by agglomerated hydroxyl functionalities.[22] Such viscoelastic behavior holds significant importance in polymers with vitrimeric and shape memory phenomena as the presence of entangled networks can be sustained even in a molten state.[23−27]

Before studying the crystallization behavior of the blends, the pristine blend components, **B**, **D**, **E**, and **F**, were subjected to thermal fractionation through Successive Self-nucleation and Annealing (SSA) measurements (Figure S8). Numerous reports describe SSA as a useful tool to determine the lamellar thickness and qualitative characterization of comonomer distribution within copolymers that crystallize over a broad temperature range.[28,29] The SSA of **B**, **D**, and **E** revealed a broad distribution of 8 distinct thermal fractions, which in each case initiates around 110 °C and terminates close to 35 °C. This great similarity derives from nearly the same sample topologies and type of branching of **B**, **D**, and **E** and is the result of using a mixture of stereoisomeric single-site catalysts, which result in a broadening of the polydispersity. Conversely, **F** displayed 6 distinct thermal fractions between 94 and 45 °C, which might be ascribed to a narrower polydispersity characteristic for a product produced by a single-site catalyst. Additionally, **F** has a well-defined peak in the high-temperature range that translates to thick and well-defined crystals, in agreement with Wide Angle X-ray Scattering (WAXS) results (Figure 5).[30] The main advantage of **B**−**E** over **F** is the capability of crystallizing over a broad temperature range, which provides better surface wetting, resulting in an improved anchoring during the bonding process.

To gain further insight into the crystal structure of **B** and its blends with the nonfunctionalized copolymers **D**−**G**, WAXS analyses were performed. All investigated copolymers displayed X-ray profiles typical for the monoclinic unit cell being characteristic for polypropylene and for this reason, the 30/70 w/w compositions **30B/70D** and **30B/70E** provided profiles resembling the corresponding pristine components (Figure 5).[31,32] The decrease of the 2θ angle values of the blends is indicative of a higher interplanar distance between polymer chains in these blends. Although TEM did not show phase separation between **B** and **F**, the poly(C_3–C_4) copolymer **F** reveals distinct crystalline morphology in comparison with **B**, **D**, and **E**. 2θ angle signals of **F** are shifted toward lower values, which is indicative for higher interplanar distances within the unit cell of the crystal in comparison with **B** and incorporation of but-1-ene chain fragments into the crystal unit cell of the polymers. In agreement with DSC analyses, we assume that the pronounced differences in unit cell dimensions between **B** and **F** impede the crystallization process within the composition (Figure 5). It is known that the existence of various types of lamella populations introduces crystalline moieties of different thermodynamic stabilities.[33] The WAXS profile of the blend **30B/70F** supports this idea since interplanar distances of unit cells are nearly identical as that of a neat **F**, while the crystallinity level is significantly diminished (13% for **30B/70F** vs 20% for **F**). Furthermore, WAXS analysis revealed the presence of the residual crystalline phase of component **G** agreeing with DSC results (Table 1, Figure S5). 2θ angle signals at 13 and 17° for **G** overlay the WAXS profile of **B** illustrating certain resemblance of lamella populations, as is supported by TEM analysis.

The effect of blending functionalized polyolefin **B** with nonfunctionalized copolymers **D**−**G** was also assessed by means of shear rheology in the linear viscoelastic regime (Figure 6). The rheological properties of sample **B** indicate that functionalization and molecular interactions significantly influence the flow behavior of these polyolefins. The presence of OH functionalities and their intermolecular interactions via hydrogen bonds provide materials displaying a low-frequency viscosity upturn as a result of the formation of "polar nests".[22,34] Diluting **B** with lower-molecular-weight **D** decreases the overall viscosity of the product, which is relevant for the processability of the HMAs. Conversely, when required, the blend's viscosity can easily be increased by mixing **B** with higher molecular weight **E**. Partial miscibility of **B** with commercially available copolymers **F** and **G**, albeit synthesized using different comonomer combination, was additionally

https://doi.org/10.1021/acs.macromol.4c02945
Macromolecules XXXX, XXX, XXX−XXX

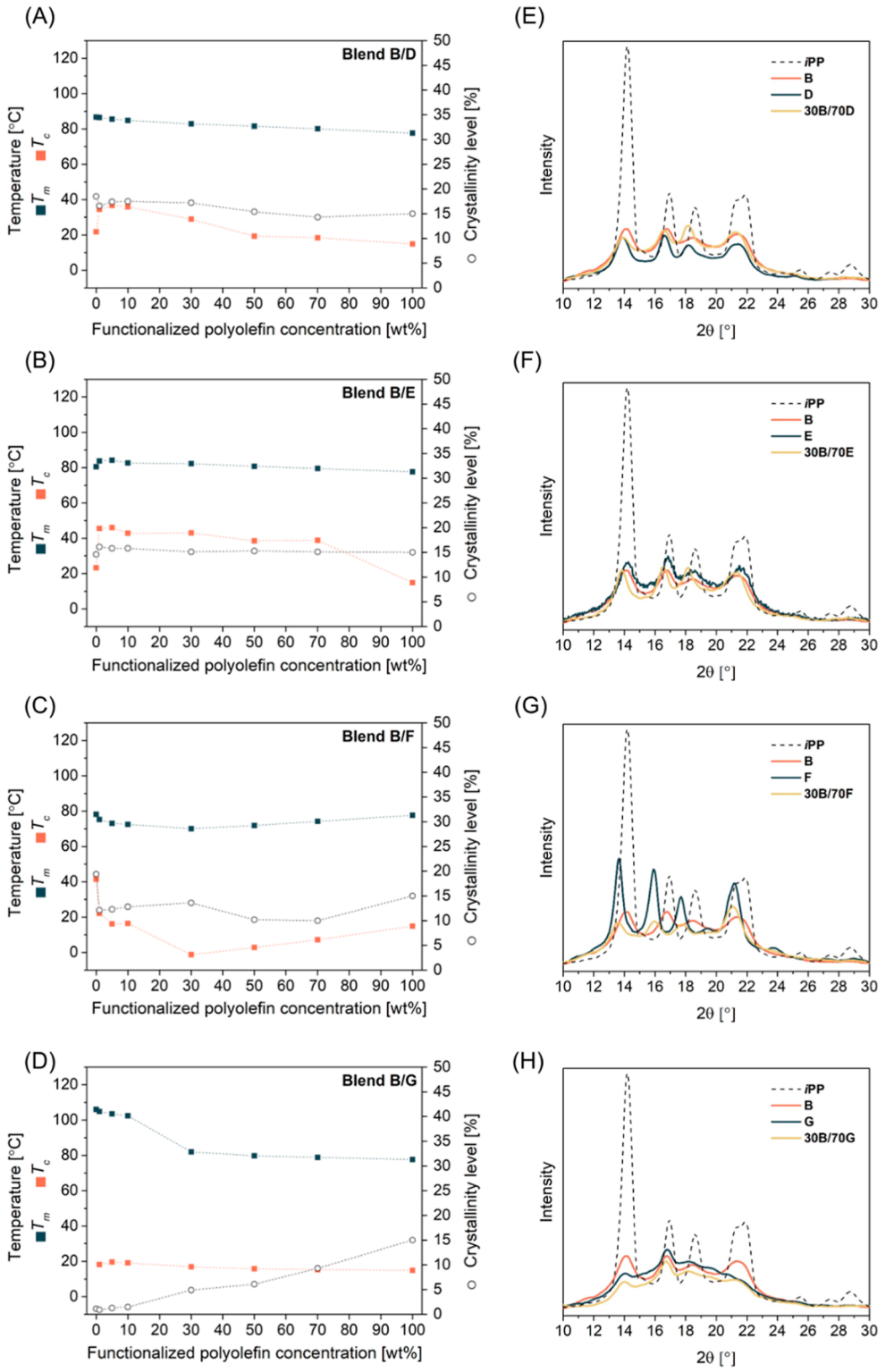

Figure 5. Melting and crystallization temperatures, crystallinity level (A–D) as well as WAXS profiles (E–H) of **B**, **D**–**G**, and blends of **B** with **D**–**G**.

proven by intact shear thinning regions for a broad range of sample compositions. Sufficient affinity between blend components is crucial for the formation of uniform phases, ensuring efficient stress transfer leading to consistent mechanical performance and optimal adhesive strength. Importantly, the presence of hydroxyl functional groups in component **B** of the investigated blends is essential for strong adhesive bond formation to aluminum or steel substrates (vide infra).

Adhesion Performance of Blends. Before assessing the performance of functionalized polyolefins and blends thereof as HMAs, the surface energies of the substrate materials steel and aluminum were compared with the polymers used as adhesives. The surface energies of steel (29 mN/m) and aluminum (42

https://doi.org/10.1021/acs.macromol.4c02945
Macromolecules XXXX, XXX, XXX–XXX

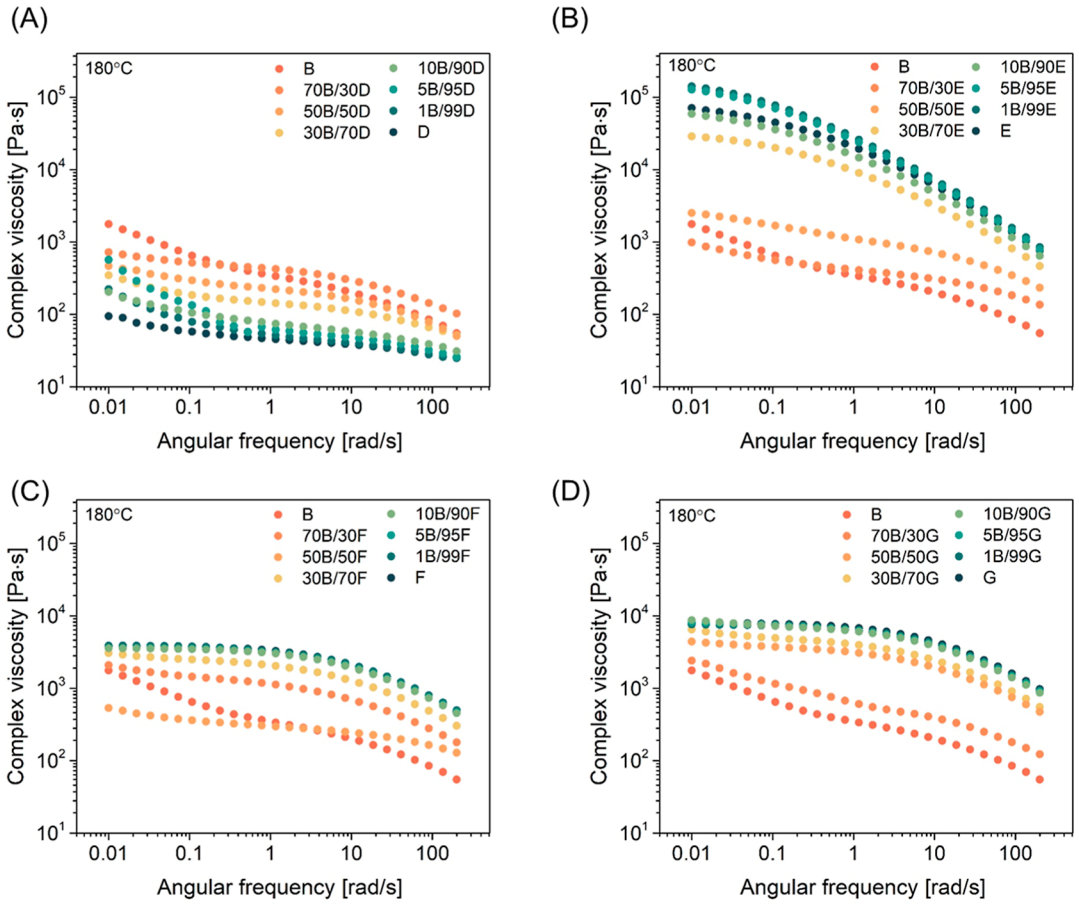

Figure 6. Complex viscosity (η^*) of polymer reference materials and blends consisting of poly(C_3−C_6−C_6OH) **B** and poly(C_3−C_6) **D**, **E** (A,B); poly(C_3−C_4) **F** (C); and poly(C_3−C_2) **G** (D). Samples were tested under oscillation frequency (ω) in a constant temperature 180 °C.

mN/m) are significantly higher than surface energies of the investigated polyolefins **B** (13 mN·m^{-1}), **D** (16 mN·m^{-1}), **E** (18 mN·m^{-1}), **F** (13 mN·m^{-1}), and **G** (17 mN·m^{-1}) (Table S3, Figure S9). The compression-molded functionalized sample **B**, prepared in a PTFE mold, revealed unexpectedly low surface energies, which can be explained by the formation of a OH polar nest in the apolar polyolefin matrix and lack of migration of the polar units to the highly apolar surface of PTFE.

Initially, lap-shear tests were performed to quantitatively asses the adhesion strength of the samples. As described above, increasing the functionality level of poly(C_3−C_6−C_6OH) from 0.1 to 0.5 mol % (**A** − **C**) resulted in a 3-fold improvement of the adhesion strength of the functionalized polyolefin to aluminum and steel (Figure 7, Table S4). Comparison of the adhesive strength and failure modes in bonding aluminum revealed two distinct regions. Where up to 3 MPa adhesive failure is dominant, above 4.5 MPa cohesive between adhesive and bonded surfaces prevails. Steel connections display mainly cohesive failures above 6 MPa. Interfacial failure, being mixed mode between adhesive and cohesive failure, is observed throughout the whole range for both aluminum and steel, respectively (Figure S10). As a comparison, the nonfunctionalized copolymers **D**−**F** revealed a negligible adhesion strength at the level of 1−2 MPa. Next, we attempted to tune the adhesion strength by diluting functionalized polyolefins with less expensive nonfunctionalized counterparts. Surprisingly, blending **B** with the nonfunctionalized congeners **D**, **E**, and **F** provided materials showing adhesive strengths that are essentially independent of the blend compositions (Figure 7, Table S4). Most striking are the results for the blends of **B** and the high-molecular-weight poly(C_3−C_6) **E** as there is—within the error of the measurement—preservation of adhesive strength despite diluting **B** 100 times! Blends of **B** with the low-molecular-weight **D** also show a constant adhesive strength independent of the blend composition but the value is somewhat lower than for neat **B**. The difference in adhesive strength between **B**/**D** and **B**/**E** blends is likely caused by the difference in the molecular weight of **D** and **E**. Low viscous, low-molecular-weight polymers tend to migrate to the surface under pressure or shear.[35] Hence, the migration of the functionalized polyolefin **B** to the surface of **B**/**E** blends is likely to be faster and more efficient than that in **B**/**D** blends. Additionally, the entanglement strength in **B**/**E** will be higher than in **B**/**D** due to the higher molecular weight of **E** as compared to that in **D**. Both effects contribute to a higher adhesive strength for the **B**/**E** system. Blends of **B** and **F** give similar results as observed for the **B**/**D** and **B**/**E** blends. Although the adhesive strength is slightly lower than that of pure **B**, the adhesive strength is independent of the blend composition ranging from **70B**/**30F** to **1B**/**99F**. Interestingly, blending of functionalized polyolefin **B** with the nonfunctionalized **G** reveals a near linear decrease in adhesion strength to both aluminum and steel with decreasing concentration of **B** (Figure 7D). For this blend, varying the blend composition can effectively be used to tune the adhesive

https://doi.org/10.1021/acs.macromol.4c02945
Macromolecules XXXX, XXX, XXX−XXX

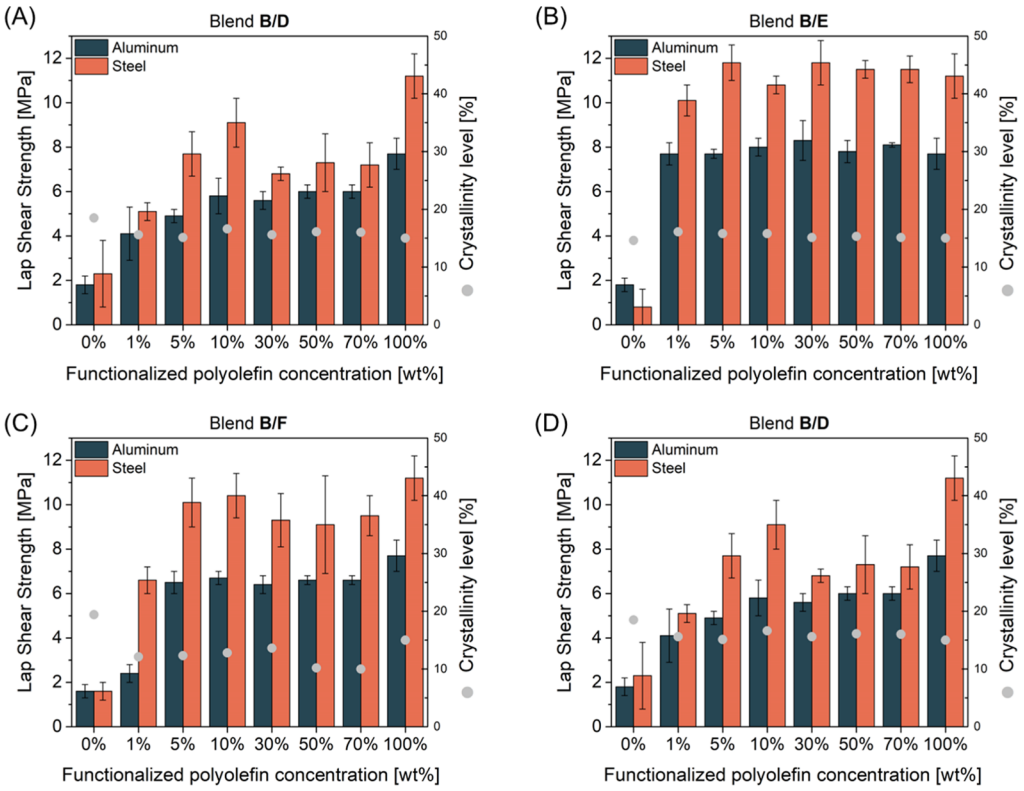

Figure 7. Lap shear test results for bonding steel and aluminum by poly(C_3–C_6–C_6OH) (**B**), poly(C_3–C_6) (**D**, **E**), poly(C_3–C_4) (**F**), poly(C_3–C_2) (**G**), and blends thereof.

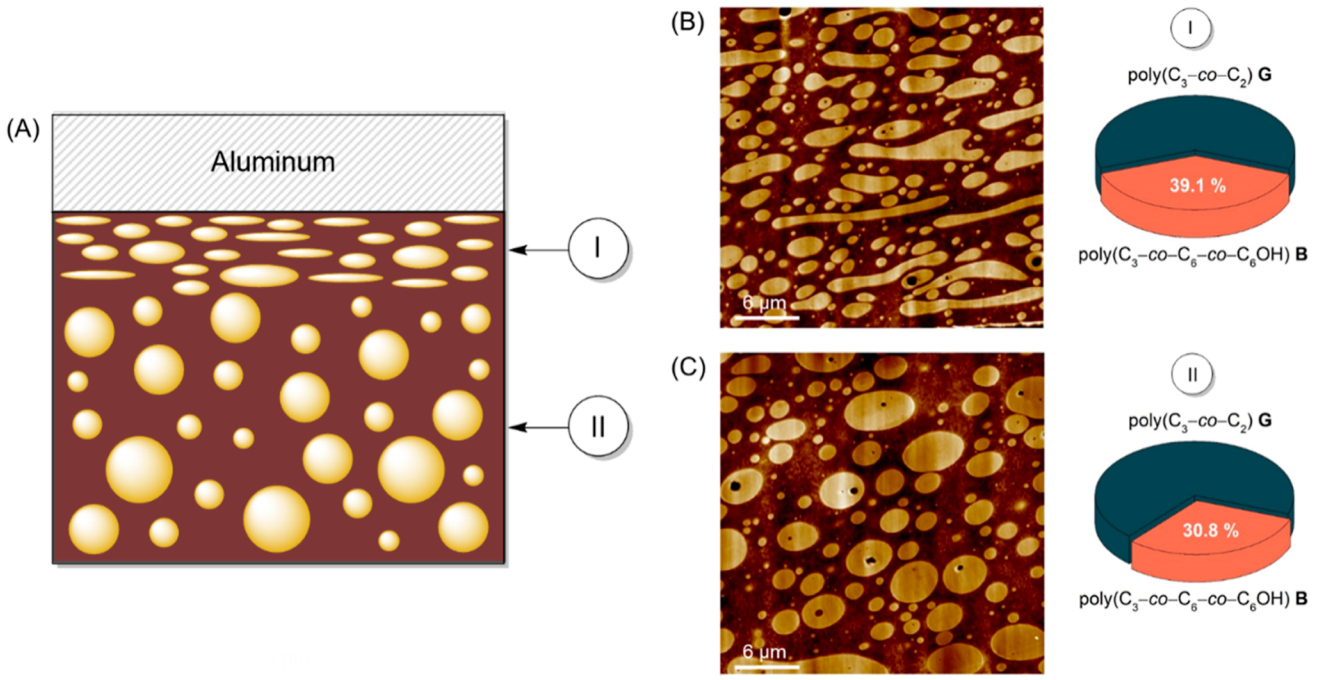

Figure 8. Graphical representation of **30B/70G** blend morphology at the interface with aluminum and core of the blend (A). AFM analysis of the **30B/70G** blend morphology at the interface with aluminum (B) and core of the blend (C).

strength of the material. The major difference between **B**, **D**–**F** and **G** is that the latter has a much lower crystallinity. Consequently, there is a proportional relationship between the **B**/**G** blend composition and the overall crystallinity and adhesion performance of the blend. A higher overall crystallinity provides a robust crystalline network which efficiently prevents deformation of the adhesives during the performance testing.[36,37] Furthermore, TEM and AFM analyses have demonstrated that blends of **B** and **D**–**F** are fully miscible, whereas **B** and **G** are at best only partly miscible. This lower miscibility and inability to cocrystallize, as is

https://doi.org/10.1021/acs.macromol.4c02945
Macromolecules XXXX, XXX, XXX–XXX

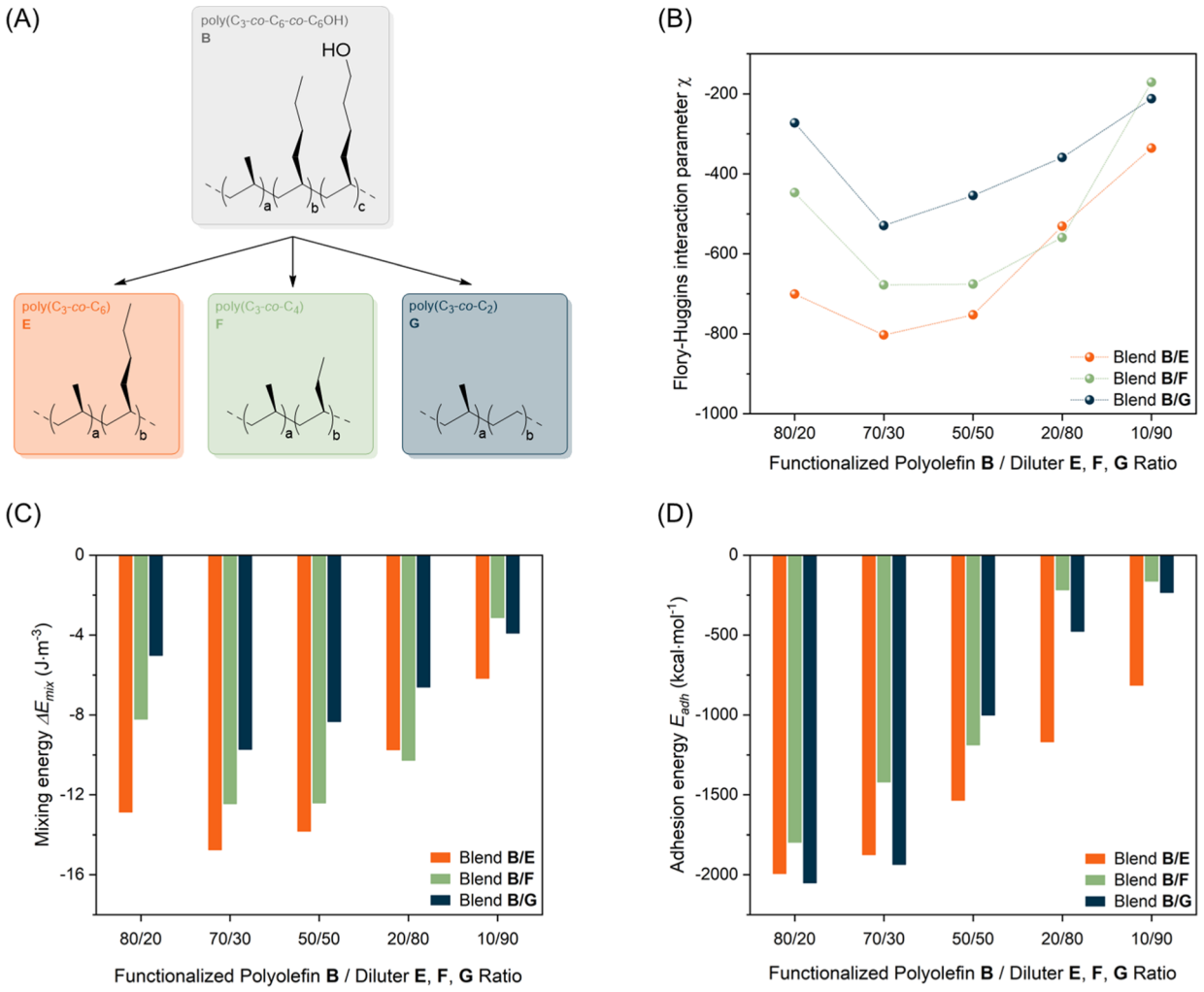

Figure 9. Structures of **B**, **E**, **F**, and **G** used in the molecular dynamics simulations (A), Flory−Huggins interaction parameter (B), Mixing Energy (C), and Adhesion Energy (D) of the five blend combinations (80:20−10:90 ratio) of each of the blend types (**B** + **E**−**G**).

possible for **B**/**D** and **B**/**E**, most likely also contributes to the different behavior of **B**/**G** blends compared to all other blends.

AFM was employed to further investigate the affinity toward polar surfaces of functionalized polyolefin within the blend (Figures 8 and S11). The **30B**/**70G** blend was chosen for the difference in the modulus of the essentially amorphous matrix **G** and semicrystalline **B** (Figure S7), which provides sufficient contrast while mapping the nanoscale morphology. In agreement with TEM analysis, also the AFM images of **30B**/**70G** reveal that **B** partly penetrates the nonfunctionalized matrix **G** (Figure 8). Notably, a clear distinction in the shape of the dispersed phase domains is observed when comparing the core of the sample with the area near the aluminum layer (Figure 8A−C). The functionalized polyolefin's domains adjacent to the aluminum layer are more elongated and densely packed compared to those in the core of the adhesive layer. Bearing analysis confirmed that near the aluminum surface, the blend is enriched with **B** (39.1 vol %), whereas the bulk of the polymer blend consists of 30.8 vol % of **B**. As mentioned earlier, this surface enrichment of **B** can be ascribed to the lower viscosity of **B** compared to **G**, but it could also be the result of an intrinsic tendency of functionalized polyolefins to migrate toward the surface of polar substrates.

Molecular dynamics simulations were used to study if the hydroxyl-functionalized polyolefins, as part of a blend with a nonfunctionalized congener, indeed tend to migrate to the interface with a polar substrate like aluminum. First, a miscibility analysis was performed to determine the affinity of **B** with the nonfunctionalized samples **E**−**G**. The miscibility of polymer blends is usually described by parameters like the Mixing Energy (ΔE_{mix})[38] and the Flory−Huggins interaction parameter (χ),[39−41] which depend on the Hildebrand solubility parameter (δ) and cohesive energy densities.[42−44] The latter can be obtained from molecular dynamics simulations.[45−48] The molecular compositions of the functionalized (**B**) and nonfunctionalized (**E**−**G**) polyolefins are given in Table S5. For each combination of **B** and **E**−**G**, we used five blend compositions (80/20, 70/30, 50/50, 20/80, and 10/90, Table S6) to comprehensively assess the impact of the composition and the compatibility (Figure 9).

Of the five **B**/**E** models, the one with a **B**/**E** ratio of 71/29 exhibits the most negative ΔE_{mix} and χ values, indicating the highest miscibility between the components. Increasing the content of **E** in the blend leads to a decrease of the ΔE_{mix} and χ values and hence the miscibility gradually decreases with increasing **E** content in the **B**/**E** blend. Similarly, also for the **B**/**F** and **B**/**G** blends, the models with a 70/30 ratio (**B**/**F** = 69.9:30.1) and **B**/**G** (70.3:29.7) demonstrate the most negative ΔE_{mix} and χ values and the miscibility gradually decreases with increasing content of **F** and **G**. Decreasing the

https://doi.org/10.1021/acs.macromol.4c02945
Macromolecules XXXX, XXX, XXX−XXX

amount of nonfunctionalized polyolefin **E**−**G** to 20 wt % resulted in a surprisingly steep increase in the ΔE_{mix} and χ values, indicating a significant decrease in miscibility with just a slight change in composition from 70:30 to 80:20 wt/wt. Taking a holistic view of ΔE_{mix} and χ data related to the best miscible models (70/30) of three different blend types (**B** + **E**−**G**) reveals an interesting trend: **B**/**E** (ΔE_{mix} = −14.74 J·m^{-3}, χ = −803.19) < **B**/**F** (ΔE_{mix} = −12.44 J·m^{-3}, χ = −677.62) < **B**/**G** (ΔE_{mix} = −9.72 J·m^{-3}, χ = −529.48). This suggests that **E** shows the highest miscibility with **B**, followed by **F**, while **G** stands at the lowest corner among the three and is in line with the expectation based on the copolymers' structures.

All five blend combinations (80:20−10:90 ratio) of each of the blend types (**B** + **E**−**G**) have been examined for their adhesion to aluminum oxide, the surface layer of an aluminum specimen (Figure 9D). In all studied blends, the functionalized polyolefin **B** is clearly located at the interface (Figure S12), indicating an intrinsic tendency of the hydroxyl-functionalized polyolefin to interact with the aluminum oxide surface, thereby improving the adhesion. For blends containing high content of **B**, the adhesion to the aluminum oxide is good for all blends regardless the type of nonfunctionalized polyolefin used. However, for blends containing lower **B** contents, the **B**/**E** blends clearly outperform the **B**/**F** and **B**/**G** blends. Since the miscibility of each of the blend types (**B**/**E**, **B**/**F**, and **B**/**G**) follows the same decreasing trend with a decreasing content of **B**, most likely the difference is caused by the higher molecular weight of **E** as compared to **F** and **G**, which might result in a preferred migration of the lower molecular weight **B** to the surface.

CONCLUSIONS

The adhesive strength of randomly hydroxyl-functionalized propylene copolymers of the type poly(propylene-*co*-hex-1-ene-*co*-hex-5-en-1-ol) to metals like aluminum or steel is impressive for an HMA. It was demonstrated that the adhesive strength of these copolymers shows a linear correlation with the hydroxyl functionality level of the copolymers, which allows the materials' adhesive strength to be tuned. However, producing many different grades with varying content of hex-5-en-1-ol is impractical for commercial-scale production of such materials. Dilution of the functionalized propylene copolymers with nonfunctionalized congeners seemed to be a simple approach to lower the average hydroxyl content in the thus obtained blend and thereby the adhesive strength. Unexpectedly, however, for blends of the functionalized poly(propylene-*co*-hex-1-ene-*co*-hex-5-en-1-ol) and the closely related nonfunctionalized poly(propylene-*co*-hex-1-ene) or poly(propylene-*co*-but-1-ene), the adhesive strength remained maintained regardless of the content of the nonfunctionalized copolymers, even for blends containing just 1 wt % of the functionalized polyolefin. Obviously, this can result in significant cost-savings for HMA production. Yet, when blends based on the low-crystalline poly(propylene-*co*-ethylene) and functionalized poly(propylene-*co*-hex-1-ene-*co*-hex-5-en-1-ol) that phase separate were tested as HMAs, a near linear drop in adhesive strength with decreasing amount of the functionalized copolymer in the blend was observed. This opens a much wider range of applications for the functionalized polyolefin as an HMA component. It is clear that the crystallinity level of the nonfunctionalized polyolefin and its miscibility with the functionalized polyolefin play a crucial role in potential to tune the adhesive strength by varying the blend composition.

ASSOCIATED CONTENT

Supporting Information

The Supporting Information is available free of charge at https://pubs.acs.org/doi/10.1021/acs.macromol.4c02945.

Additional experimental details, molecular dynamics modeling details, materials, methods, surface characterization and ^{1}H NMR, SEC, DSC, WAXS, AFM, DMA, rheology, and lap shear tests (PDF)

AUTHOR INFORMATION

Corresponding Authors

Lidia Jasinska-Walc − *Department of Chemistry and Technology of Functional Materials, Chemical Faculty, Gdansk University of Technology, 80-233 Gdansk, Poland; SABIC Technology & Innovation, 6167 RD Geleen, The Netherlands;* orcid.org/0000-0001-6793-6936; Email: Lidia.Jasinska-Walc@SABIC.com

Rob Duchateau − *Chemical Product Engineering, Department of Chemical Engineering, University of Groningen, 9747 AG Groningen, The Netherlands; SABIC Technology & Innovation, 6167 RD Geleen, The Netherlands;* orcid.org/0000-0002-2641-4354; Email: R.Duchateau@RUG.nl

Authors

Jakub Kruszynski − *Department of Chemistry and Technology of Functional Materials, Chemical Faculty, Gdansk University of Technology, 80-233 Gdansk, Poland; SABIC Technology & Innovation, 6167 RD Geleen, The Netherlands;* orcid.org/0000-0003-0908-2586

Weronika Nowicka − *Department of Chemistry and Technology of Functional Materials, Chemical Faculty, Gdansk University of Technology, 80-233 Gdansk, Poland; SABIC Technology & Innovation, 6167 RD Geleen, The Netherlands;* orcid.org/0009-0002-3681-3102

Farhan Ahmad Pasha − *SABIC Technology Center at KAUST, 23955 Thuwal, Saudi-Arabia;* orcid.org/0000-0002-7132-6361

Lanti Yang − *SABIC Technology & Innovation, 4612 PX Bergen op Zoom, The Netherlands*

Artur Rozanski − *Centre of Molecular and Macromolecular Studies, Polish Academy of Sciences, 90-363 Lodz, Poland*

Miloud Bouyahyi − *SABIC Technology & Innovation, 6167 RD Geleen, The Netherlands;* orcid.org/0000-0001-7466-6671

Ralf Kleppinger − *SABIC Technology & Innovation, 6167 RD Geleen, The Netherlands*

Complete contact information is available at: https://pubs.acs.org/10.1021/acs.macromol.4c02945

Author Contributions

¶The contribution of J.K. and W.N. is equal.

Funding

This research was funded by SABIC.

Notes

The authors declare no competing financial interest.

■ ACKNOWLEDGMENTS

Authors thank Sebastien Pierrat and Fleur Vanosch for the analytical and rheological support.

■ ABBREVIATIONS

VOC: volatile organic compound; EVA: ethylene-vinyl alcohol copolymer; PTFE: polytetrafluoroethylene

■ REFERENCES

(1) Heucher, R.; Ford, I.; Joseph, J.; Crawford, A. Debondable reactive hot melt adhesives U.S. Patent 10,800,956 B2, 2020.
(2) Kruszynski, J.; Nowicka, W.; Bouyahyi, M.; Liu, Y.; Yang, L.; Rozanski, A.; Anbuchezhian, N.; Jasinska-Walc, L.; Duchateau, R. Unprecedented Adhesive Performance of Propylene-Based Hydroxyl-Functionalized Terpolymers. *ACS Appl. Polym. Mater.* **2023**, *5* (5), 3875−3882.
(3) Li, W.; Bouzidi, L.; Narine, S. S. Current Research and Development Status and Prospect of Hot-Melt Adhesives: A Review. *Ind. Eng. Chem. Res.* **2008**, *47* (20), 7524−7532.
(4) Herbert, K. M.; Dolinski, N. D.; Boynton, N. R.; Murphy, J. G.; Lindberg, C. A.; Sibener, S. J.; Rowan, S. J. Controlling the Morphology of Dynamic Thia-Michael Networks to Target Pressure-Sensitive and Hot Melt Adhesives. *ACS Appl. Mater. Interfaces* **2021**, *13* (23), 27471−27480.
(5) Awaja, F.; Gilbert, M.; Kelly, G.; Fox, B.; Pigram, P. J. Adhesion of polymers. *Prog. Polym. Sci.* **2009**, *34* (9), 948−968.
(6) Raos, G.; Zappone, B. Polymer Adhesion: Seeking New Solutions for an Old Problem. *Macromolecules* **2021**, *54* (23), 10617−10644.
(7) Khairullin, I. K. Adhesive-melts-the most dynamically developing area in world production and consumption of adhesives. *Polym. Sci., Ser. D* **2013**, *6* (1), 77−81.
(8) Jozef, R.; Lyda, R.; Igor, N.; Vladimír, V.; Jozef, P.; Ivica, J.; Ivan, C. Thermooxidative stability of hot melt adhesives based on metallocene polyolefins grafted with polar acrylic acid moieties. *Polym. Test.* **2020**, *85*, 106422.
(9) Sun, P.; Li, Y.; Qin, B.; Xu, J.-F.; Zhang, X. Super Strong and Multi-Reusable Supramolecular Epoxy Hot Melt Adhesives. *ACS Mater. Lett.* **2021**, *3* (7), 1003−1009.
(10) Rahman, M. A.; Bowland, C.; Ge, S.; Acharya, S. R.; Kim, S.; Cooper, V. R.; Chen, X. C.; Irle, S.; Sokolov, A. P.; Savara, A.; et al. Design of tough adhesive from commodity thermoplastics through dynamic crosslinking. *Sci. Adv.* **2021**, *7* (42), No. eabk2451.
(11) Jasinska-Walc, L.; Duchateau, R.; Bouyahyi, M.; Badillo Sampedro, N.; Kruszynski, J.; Hrachova, J.; Liu, Y.; Yang, L. Hot melt adhesive comprising functionalized polyolefins. U.S. Patent 20,240,263,052 A1, 2022.
(12) Jasinska-Walc, L.; Duchateau, R.; Bouyahyi, M.; Kruszynski, J.; Gautam, P. S.; Nowicka, W.; Szot, W. Hot Melt Adhesives Based on Blends Comprising Non-Functionalized and Functionalized Polyolefins. WO 2025002627 A1, 2025.
(13) Ahagon, A.; Gent, A. N. Effect of interfacial bonding on the strength of adhesion. *J. Polym. Sci., Polym. Phys. Ed.* **1975**, *13* (7), 1285−1300.
(14) Matsumoto, T.; Shimizu, Y.; Nishino, T. Analyses of the Adhesion Interphase of Isotactic Polypropylene Using Hot-Melt Polyolefin Adhesives. *Macromolecules* **2021**, *54* (15), 7226−7233.
(15) Boutar, Y.; Naïmi, S.; Mezlini, S.; da Silva, L. F. M.; Hamdaoui, M.; Ben Sik Ali, M. Effect of adhesive thickness and surface roughness on the shear strength of aluminium one-component polyurethane adhesive single-lap joints for automotive applications. *J. Adhes. Sci. Technol.* **2016**, *30* (17), 1913−1929.
(16) Washiyama, J.; Kramer, E. J.; Hui, C. Y. Fracture mechanisms of polymer interfaces reinforced with block copolymers: transition from chain pullout to crazing. *Macromolecules* **1993**, *26* (11), 2928−2934.
(17) Creton, C.; Brown, H. R.; Deline, V. R. Influence of Chain Entanglement on the Failure Modes in Block Copolymer Toughened Interfaces. *Macromolecules* **1994**, *27* (7), 1774−1780.
(18) Lyu, L.; Ohnuma, Y.; Shigemoto, Y.; Hanada, T.; Fukada, T.; Akiyama, H.; Terasaki, N.; Horiuchi, S. Toughness and Durability of Interfaces in Dissimilar Adhesive Joints of Aluminum and Carbon-Fiber-Reinforced Thermoplastics. *Langmuir* **2020**, *36* (46), 14046−14057.
(19) Merkx, M. J. M.; Angelidis, A.; Mameli, A.; Li, J.; Lemaire, P. C.; Sharma, K.; Hausmann, D. M.; Kessels, W. M. M.; Sandoval, T. E.; Mackus, A. J. M. Relation between Reactive Surface Sites and Precursor Choice for Area-Selective Atomic Layer Deposition Using Small Molecule Inhibitors. *J. Phys. Chem. C* **2022**, *126* (10), 4845−4853.
(20) Pepels, M. P. F.; Kleijnen, R. G.; Goossens, J. G. P.; Spoelstra, A. B.; Tandler, R.; Martens, H.; Soliman, M.; Duchateau, R. Compatibility and epitaxial crystallization between Poly(ethylene) and Poly(ethylene)-like polyesters. *Polymer* **2016**, *88*, 63−70.
(21) Thirtha, V.; Lehman, R.; Nosker, T. Morphological effects on glass transition behavior in selected immiscible blends of amorphous and semicrystalline polymers. *Polymer* **2006**, *47* (15), 5392−5401.
(22) Wouters, M. E. L.; Goossens, J. G. P.; Binsbergen, F. L. Morphology of Neutralized Low Molecular Weight Maleated Ethylene−Propylene Copolymers (MAn-g-EPM) As Investigated by Small-Angle X-ray Scattering. *Macromolecules* **2002**, *35* (1), 208−216.
(23) Maaz, M.; Riba-Bremerch, A.; Guibert, C.; Van Zee, N. J.; Nicolaÿ, R. Synthesis of Polyethylene Vitrimers in a Single Step: Consequences of Graft Structure, Reactive Extrusion Conditions, and Processing Aids. *Macromolecules* **2021**, *54* (5), 2213−2225.
(24) Xi Wang, T.; Mei Chen, H.; Li, T.; Siang Lucas Ng, B.; Xie, H.; Xiao, R.; Min Huang, W. Tan-delta plateau in vitrimer-like polyurethanes. *Mater. Lett.* **2022**, *325*, 132884.
(25) Balzade, Z.; Sharif, F.; Ghaffarian Anbaran, S. R. Tailor-Made Functional Polyolefins of Complex Architectures: Recent Advances, Applications, and Prospects. *Macromolecules* **2022**, *55* (16), 6938−6972.
(26) Odenwald, L.; Wimmer, F. P.; Mast, N. K.; Schußmann, M. G.; Wilhelm, M.; Mecking, S. Molecularly Defined Polyolefin Vitrimers from Catalytic Insertion Polymerization. *J. Am. Chem. Soc.* **2022**, *144* (29), 13226−13233.
(27) Ahmadi, M.; Hanifpour, A.; Ghiassinejad, S.; van Ruymbeke, E. Polyolefins Vitrimers: Design Principles and Applications. *Chem. Mater.* **2022**, *34* (23), 10249−10271.
(28) Müller, A. J.; Arnal, M. L. Thermal fractionation of polymers. *Prog. Polym. Sci.* **2005**, *30* (5), 559−603.
(29) Müller, A. J.; Michell, R. M.; Pérez, R. A.; Lorenzo, A. T. Successive Self-nucleation and Annealing (SSA): Correct design of thermal protocol and applications. *Eur. Polym. J.* **2015**, *65*, 132−154.
(30) Urciuoli, G.; Ruiz de Ballesteros, O.; Cipullo, R.; Trifuoggi, M.; Giarra, A.; Auriemma, F. Thermal Fractionation of Ethylene/1-Octene Multiblock Copolymers from Chain Shuttling Polymerization. *Macromolecules* **2022**, *55* (13), 5656−5668.
(31) Androsch, R.; Wunderlich, B. Reversible Crystallization and Melting at the Lateral Surface of Isotactic Polypropylene Crystals. *Macromolecules* **2001**, *34* (17), 5950−5960.
(32) De Rosa, C.; Dello Iacono, S.; Auriemma, F.; Ciaccia, E.; Resconi, L. Crystal Structure of Isotactic Propylene−Hexene Copolymers: The Trigonal Form of Isotactic Polypropylene. *Macromolecules* **2006**, *39* (18), 6098−6109.
(33) Duan, Y.; Zhang, J.; Shen, D.; Yan, S. In Situ FTIR Studies on the Cold-Crystallization Process and Multiple Melting Behavior of Isotactic Polystyrene. *Macromolecules* **2003**, *36* (13), 4874−4879.
(34) Ricarte, R. G.; Tournilhac, F.; Leibler, L. Phase Separation and Self-Assembly in Vitrimers: Hierarchical Morphology of Molten and Semicrystalline Polyethylene/Dioxaborolane Maleimide Systems. *Macromolecules* **2019**, *52* (2), 432−443.
(35) Lee, B. L.; White, J. L. An Experimental Study of Rheological Properties of Polymer Melts in Laminar Shear Flow and of Interface

https://doi.org/10.1021/acs.macromol.4c02945
Macromolecules XXXX, XXX, XXX−XXX

Deformation and Its Mechanisms in Two-Phase Stratified Flow. *Trans. Soc. Rheol.* **1974**, *18* (3), 467−492.
(36) Nakao, K. Relationship Between Bond Strength and Crystallinity of High Polymers-Polyethylene, Polyethyleneterephthalate, and Nylon. *J. Adhes.* **1972**, *4* (2), 95−108.
(37) Hoecker, F.; Karger-Kocsis, J. Effects of crystallinity and supermolecular formations on the interfacial shear strength and adhesion in GF/PP composites. *Polym. Bull.* **1993**, *31* (6), 707−714.
(38) Gomes, A. D. S. *Polymerization*; IntechOpen: Rijeka, 2012.
(39) Abou-Rachid, H.; Lussier, L.-S.; Ringuette, S.; Lafleur-Lambert, X.; Jaidann, M.; Brisson, J. On the Correlation between Miscibility and Solubility Properties of Energetic Plasticizers/Polymer Blends: Modeling and Simulation Studies. *Propellants, Explos., Pyrotech.* **2008**, *33* (4), 301−310.
(40) Ahmadi, A.; Freire, J. J. Molecular dynamics simulation study of compatibility for the polyvinylmethylether/polystyrene mixture. *Mol. Simul.* **2008**, *34* (10−15), 1253−1258.
(41) Cui, X. W.; Zhang, L. Amorphous State and Solubility Simulation of Poly(N-arylenebenzimidazole ketone). *Appl. Mech. Mater.* **2014**, *513*−*517*, 295−298.
(42) Gestoso, P.; Brisson, J. Orientation of uniaxially stretched poly(vinyl phenol)/poly(vinyl methyl ether) blends. *Polymer* **2001**, *42* (20), 8415−8424.
(43) Gestoso, P.; Brisson, J. Effect of hydrogen bonds on the amorphous phase of a polymer as determined by atomistic molecular modelling. *Comput. Theor. Polym. Sci.* **2001**, *11* (4), 263−271.
(44) Zhang, M.; Choi, P.; Sundararaj, U. Molecular dynamics and thermal analysis study of anomalous thermodynamic behavior of poly (ether imide)/polycarbonate blends. *Polymer* **2003**, *44* (6), 1979−1986.
(45) Tambasco, M.; Lipson, J. E. G.; Higgins, J. S. Blend Miscibility and the Flory−Huggins Interaction Parameter: A Critical Examination. *Macromolecules* **2006**, *39* (14), 4860−4868.
(46) Gupta, J.; Nunes, C.; Vyas, S.; Jonnalagadda, S. Prediction of Solubility Parameters and Miscibility of Pharmaceutical Compounds by Molecular Dynamics Simulations. *J. Phys. Chem. B* **2011**, *115* (9), 2014−2023.
(47) Guo, Y.; Liu, J.; Lu, Y.; Dong, D.; Wang, W.; Zhang, L. A combined molecular dynamics simulation and experimental method to study the compatibility between elastomers and resins. *RSC Adv.* **2018**, *8* (26), 14401−14413.
(48) Lebga-Nebane, J. L.; Sankarasubramanian, M.; Chojecki, G.; Ning, B.; Yuya, P. A.; Moosbrugger, J. C.; Rasmussen, D. H.; Krishnan, S. Polyetheretherketone hexagonal boron nitride, and tungsten carbide cobalt chromium composite coatings: Mechanical and tribological properties. *J. Appl. Polym. Sci.* **2021**, *138* (21), 50504.

https://doi.org/10.1021/acs.macromol.4c02945
Macromolecules XXXX, XXX, XXX−XXX